CFD Investigation and Aerodynamic Analysis of a Small-Scale Horizontal Axis Wind Turbine Performance Customized to Suit the Climate Conditions of Mosul City

Yaser MAHMOOD
Mechanical Engineering Department, College of Engineering, University of Mosul, Mosul, 41002, Iraq; Laboratory of Mechanics, Modeling and Productivity (LA2MP), National School of Engineers of Sfax, University of Sfax, BP N ° 1173 - 3038, Sfax, Tunisia, yaseralmola@uomosul.edu.iq

Mohamed TAKTAK *
Laboratory of Mechanics, Modeling and Productivity (LA2MP), National School of Engineers of Sfax, University of Sfax, BP N ° 1173 - 3038, Sfax, Tunisia, mohamed.taktak@fss.usf.tn

Mohamed HADDAR
Laboratory of Mechanics, Modeling and Productivity (LA2MP), National School of Engineers of Sfax, University of Sfax, BP N ° 1173 - 3038, Sfax, Tunisia, mohamed.haddar@enis.usf.tn

* Author to whom correspondence should be addressed

Abstract: - This paper offers detailed CFD research and aerodynamics of a small-scale HAWT relevant to the meteorological circumstances in Mosul City. This current work shows the best way of building a wind turbine blade using the BEM Theory as the basis. The blade was subdivided into twenty parts along the blade span to form the elements of the blade. The chord length and twist angle distributions over the span were estimated at each section normal to the blade length. Findings show effectiveness in the enhancement of energy retrieval and system stability, thus proving the possibility of optimizing turbines for renewable energy production in the city environment. As highlighted in the CFD findings conditions, the power coefficient is related to the incoming wind speed at a constant rate of the rotor speed. The power coefficient increases with the tip speed ratio up to a certain point, after which it decreases and eventually approaches zero as the tip speed ratio continues to rise. The power coefficient is maximum at a value of 0.35 at a tip-speed ratio of 3.5. As a result of the present design of HAWT, it offers the ability to operate in the low-speed wind regions.

Keywords: - CFD, Design of wind turbine, Horizontal axis wind turbine, Aerodynamic, Mosul city.

1. INTRODUCTION

Global warming and the subsequent changes in climate, as well as the emission of greenhouse gases as a result of burning carbon-based energies, make it critical for the world to change its energy sources. It is necessary to move away from the current state of affairs to reduce harm to the environment and ensure effective energy utilization. As a result, more attention is paid to pursuing other types of energy, especially bearing in mind the development of renewable energy sources for research [1]. But in the case of elective sources of energy, wind energy is different due to availability, cost, flexibility, and satisfaction of the energy demand with the least emission of carbon in the world. Hence, it could be deduced that the advancement and international expansion of wind generation structures have been quite impressive. As for wind, it also experienced a very rapid increase; the total installed wind power reached 742GW by the reference of the year 2020. Windmills are structures that are put up with pre-disposing attributes that would create a harbor to generate electricity from the kinetic energy of the wind. It is also possible to note that the efficiency of such turbines is determined by the wind speed, air density, and geometrical parameters of the blades. Blade design, therefore, forms one of the paramount aspects that define the efficiency in the generation of electricity, just as it helps to limit the costs in manufacturing expenses [2, 3].

Researchers are also working hard to tweak blade designs in a bid to enhance obtained outcomes that are produced through the simulation of the wind. In

regard to wind turbine output, there are certain factors that range from the wind speed, the density of air, or the outline and dimensions of the blades. The nature of the operation of turbine blades involves capturing wind energy and converting it into mechanical energy [4]. Therefore, the design of these blades is crucial regarding more than fifty percent of the amount of swept space of the wind and is equipped to withstand these wind loads. These were speed and direction, which are the main determinants of behavior in relation to the turbines.

Turbine power output thereby has a direct proportional relationship with higher wind speeds. This is because with increased wind velocity, there will be more kinetic energy that can be utilized by the turbine blades [5, 6]. However, they must operate optimally based on the two explicit wind speeds labeled as the cut-in and the cut-out. Cut-in speed is the lowest speed at which the turbine can start generating power, and its average range is between 3-4 m/s, while the cut-out speed is the maximum speed that the turbine can operate without getting damaged and may range between 20-25 m/s [7].

Researchers are also working hard to tweak blade designs in a bid to enhance obtained outcomes that are produced through the simulation of the wind. In regard to wind turbine output, there are certain factors that range from the wind speed, the density of air, or the outline and dimensions of the blades. The nature of the operation of turbine blades involves capturing wind energy and converting it into mechanical energy [8]. Therefore, the design of these blades is crucial with regard to more than fifty percent of the amount of swept space of the wind, and is equipped to withstand these wind loads. These were speed and direction, which are the main determinants of behavior in relation to the turbines. Turbine output power thereby has a direct proportional relationship with higher wind speeds this is because with increased wind velocity, there will be more kinetic energy that can be utilized by the turbine blades [9].

Wind turbines must operate optimally within specific wind speed ranges, defined by the cut-in and cut-out speeds. The cut-in speed, typically between 3–4 m/s, is the minimum wind speed required for the turbine to start generating power. The cut-out speed, generally ranging between 20–25 m/s, is the maximum wind speed at which the turbine can operate safely without risking damage. Several design features, such as tapered blade tips and optimized airfoil shapes, play a critical role in minimizing turbulence and noise while enhancing efficiency.

Wind tunnel experiments and field data have demonstrated significant potential for improving energy capture and overall turbine performance through small modifications to blade geometry. For instance, Roshin Ahmed and Mahdi Abdel Hussein [11] utilized MATLAB-Simulink to model and simulate wind turbines. Their mathematical model analyzed power generation in relation to key parameters such as wind speed, air density, power coefficient, blade pitch angle, and tip speed. The study revealed that turbine efficiency is strongly influenced by wind flow speed and air density—factors that are, in turn, affected by temperature. The authors emphasized MATLAB-Simulink's graphical environment as an effective tool for modeling and simulating dynamic systems, making it particularly useful for wind turbine design and analysis [10]. Development in wind turbine blades is always trying to improve the structure design in relation to its performance. The two methods applied most often to study and predict the effect of blade motions under different wind conditions are CFD and wind tunnel tests. It turned out that the ratio of blade angle, as well as using flexible materials, can increase the yield of energy captured and decrease the mechanical load on the structure [11].

The innovations that are currently under investigation include; the adaptive blade technologies whereby the blades are able to change their profile so as to operate in different wind conditions, as this supports increased efficiency and durability. Cole J. Daves from Colorado State University presented a paper on the modeling of wake effects of wind turbines in 2012. A description of the usage of turbulence methods in the context of Computational Fluid Dynamics (CFD) is provided using the model of NREL 5MW turbine developed in SolidWorks and ANSYS Design Modeler. The study pointed out the degree and capacities that can be attained in desktop computing, establishing it as pivotal to learners and the magnification of wind energy systems. Also, Abdullah et al. [12] presented a research work on modeling and simulations of 1. The facts related to this type include 5-megawatt variable-speed wind turbines that have dominated the current market. They explored two control strategies: used for varying the rotor speed at low wind conditions for the highest possible efficiency, and to vary the blade pitch angle at high wind conditions for optimum rotational speed. The analysis made it clear that power output depends on the wind speed and turbine speed, and the fact that the power output is affected by turbulence. The simulations were carried out using Matlab/Simulink, where emphasis was done to a turbine with a rated power of 1. 5 MW.

In 2006, Alpinar and colleagues conducted a comprehensive evaluation of wind turbine performance and wind energy potential across four regions in Turkey: Maden, Ağın, Elazığ, and Keban.

They estimated the energy production capabilities of six wind turbines, with capacities of 300, 600, 900, 1200, 1800, and 2300 kilowatts, using wind speed and direction data collected between 1998 and 2003. Their studies show that the best places to install wind turbines are where there is the most frequent wind availability in order to obtain the most output and reliability from the turbines. Moreover, in the theoretical works, Camelia and his group [13] presented a Modeling, simulation, and monitoring of wind turbines. They focused on the four key elements of a turbine system: the wind, the wind turbine, the stator of the alternating current generator, and the control device. The objective of the work was the construction of a mathematical model of wind turbines, their simulation, and the creation of a control unit for the implementation of wind energy in a home setting. Inspecting and simulating each part, components, and models; the integration and testing of the total system were also done. The experiment results verified the rationality of the above mathematical models for the engineering applications by using the simulation results as a reference in order to improve the system design.

Salih et. al. [14] analyzed wind turbine performance under various factors using simulation models. They used MATLAB to study small energy systems and evaluated two wind turbines: Whisper-500 3.2KW and NY- WSR1204 600W. Their findings showed that air properties, such as wind speed, air density, pressure, temperature, and power factor, significantly impact turbine power generation. Increased wind speed and density enhance production, while higher temperatures reduce it, guiding future research and development priorities. In 2012, researcher Zijun Zhang [15] conducted a study to enhance wind turbine performance through effective control strategies aimed at reducing power generation costs. Traditional physics-based models of wind turbines, which include mechanical, electrical, and software components, are often complex and inaccurate. With advancements in data acquisition, large amounts of wind energy data can now be collected and analyzed. Zhang applied data mining and created accurate, data-driven models of wind turbines. The study focused on optimizing wind turbines and wind farms to improve performance and reduce operational costs. The methodology proposed is applicable across the wind industry.

On the other hand, Rodrigues and Rossi [16] compared the electricity production of small wind turbines using the (HOMER) program, where wind turbines were simulated through the (HOMER) program from the perspective of wind resources in three different cities, two of which were in Brazil and one In the United States, the results indicate that energy costs depend on wind turbine characteristics (technical and operational characteristics of wind turbines), such that maximum energy production can be achieved.

Wiratama et. al. [17] conducted a study to investigate the factors affecting wind turbine capacity in Indonesia. They focused on how wind speed and air density enhance energy capture. The study concluded that higher air density and wind speed significantly increase energy generation, with energy output proportional to the cube of wind speed. Additionally, altitude and temperature influence these factors, with lower temperatures enhancing the power curve and energy output. These findings are useful in the identification of suitable and more productive wind turbines considering certain sites.

Moreover, research was carried out by Samah Shia & Muhammad Abdullah [18] on Wind Energy at Tuz Khurmatu. Their research was to find out whether it is possible to set up a wind farm in Tuz Khurmatu, Iraq, at different heights, which they established to be most appropriate. The proposed wind farm includes: Nordex N29, Nordex N43, and Enercon-33. The study also established that at a height of 10 meters, wind speed varies from 3.14 m/s and 3. The speed of the first climber is recorded at 26 m/s when at 40 meters, and for the second climber speed is recorded at 4 m/s when at 40 meters. 86 m/s. The area in Tuz Khurmatu has a low wind power class, meaning that the wind speed is low and suitable only for low-speed wind turbines.

Moreover, Esraa A. Mansoor [19] also performed a practical achievement concerning the efficiency of a horizontal-axis wind turbine at the real site in Kirkuk. This research focused on the use of wind turbines in delivering clean energy with regard to the effects of temperature, wind speed, direction, and dust concentration. A 400W turbine at a height of 16m was used, and data was collected during summer and winter. The results, analyzed using MATLAB, showed that summer had better energy production (100724 kW.hr monthly average) compared to winter (9552.5 kW.hr) due to higher wind speeds in summer. High temperatures and humidity were found to inversely affect turbine power, while dust had a minimal impact. The study found a power factor of 0.37 and established a polynomial relationship between wind speed and generated power.

Previous studies, such as those by Samah Shia and Muhammad Abdullah, and Esraa A. Mansoor, have laid the groundwork for understanding wind energy potential in various regions of Iraq. Shia and Abdullah's preliminary survey in Tuz Khurmatu explored the feasibility of wind farms at different altitudes, highlighting the suitability of low-speed wind turbines in the region. Similarly, in Mansoor’s

matters of fact and real site measurement study in Kirkuk, the efficiency of the horizontal axis wind turbine was investigated for the selected aerophysical parameter under actual site range climate conditions, such as temperature, wind velocity, density of dust etc.

Recent advancements have further expanded the scope of wind turbine design and optimization, focusing on both macro- and micro-scale factors affecting performance. Innovations such as smart sensors and data-driven algorithms now allow for real-time performance monitoring, optimizing power generation through adaptive control strategies. Studies have demonstrated that leveraging artificial intelligence and machine learning can significantly enhance turbine efficiency by predicting wind patterns, adjusting blade angles dynamically, and minimizing downtime due to maintenance needs [20]. These approaches help improve the overall reliability and cost-effectiveness of wind power systems.

Additionally, a growing body of work emphasizes site-specific considerations in wind energy deployment. [21] showed that wind speed, air density, and altitude can greatly influence energy capture, guiding decisions on turbine placement and design for maximum output. Similarly, [22] regional analyses have revealed critical insights into localized wind energy potential, emphasizing that optimal site selection and turbine customization can yield substantial improvements in energy production. These findings underline the importance of integrating environmental and geographic factors into wind energy planning to maximize the technology's effectiveness and reliability.

Computational Fluid Dynamics (CFD) involves the study and analysis of fluid flows through numerical solutions to systems of partial differential equations (PDEs). Initially adopted by the aerospace industry, CFD has since broadened its applications across various sectors, driven by advancements in computational power and significant economic benefits.

Extensive experimental studies of fluid flows are often costly and time-consuming, making Computational Fluid Dynamics (CFD) invaluable across various industries, including the wind power sector. CFD enables the examination of idealized scenarios that are impractical to replicate, as well as phenomena on extremely small scales and their temporal evolution, which would otherwise be invisible. Given the complexity of the equations governing fluid dynamics, computational methods are employed to solve these problems. Furthermore, there is a large area of study regarding the usage of CFD in the design and optimization of mini-Small HAWTs designed for Mosul's specific meteorological characteristics. These opportunities include how to improve the CFD in order to predict the turbine performance under the different local wind conditions and where to find an adequate systematic design approach integrating these predictions into realistic turbines. Filling this gap is important for the progress of offering appropriate and resourceful wind energy solutions in Mosul and other areas with similar weather patterns.

Therefore, the current work distinguishes itself by providing a context-specific design optimization for Mosul, Iraq, where wind resources are limited (1–6 m/s). Unlike prior efforts that focus on general models or higher wind velocity sites, this study directly addresses the challenges of low wind speeds by applying Computational Fluid Dynamics (CFD) to develop a customized small-scale Horizontal Axis Wind Turbine (HAWT) tailored for Mosul's actual meteorological data. While previous works used simulation tools in standard settings, this research goes further by:

1-Integrating localized meteorological data (e.g., wind speed distribution, temperature, dust concentration) into the turbine design process.

2-Using CFD not only for performance prediction, but also as a design tool to fine-tune the blade profile for low-speed, high-efficiency operations.

3-Providing a practical, small-scale renewable energy solution for regions with similar wind patterns, where large-scale commercial turbines would be inefficient.

2. MOSUL METEOROLOGICAL DATA

A study on the climatology of Ninawa Province, Iraq, revealed significant variations in wind speed across the region. The findings indicate that southern areas of Ninawa, such as the Jabal Sinjar region, experience relatively higher wind velocities, with speeds reaching up to 9 m/s.

Wind speeds of 5 m/s are generally considered suitable for wind energy harvesting, as illustrated in Figures 1 and 2. In contrast, Mosul, the capital of Ninawa Province, has lower wind potential, with wind speeds ranging from 1 m/s to 6 m/s. This limited wind resource poses challenges for the optimal placement of wind turbines in Mosul.

To address these challenges, solutions such as Computational Fluid Dynamics (CFD) have been proposed. CFD enables the design of turbines optimized for low wind speeds, improving their ability to convert available wind energy into electricity.

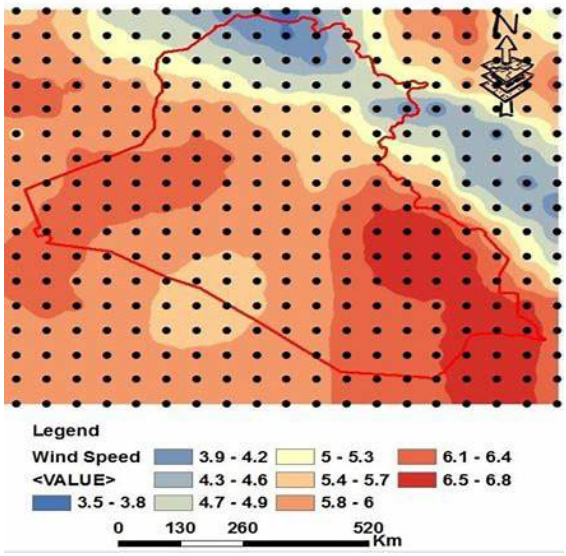

Figure 1. Global Distribution of Wind Speeds Across Iraq [36]

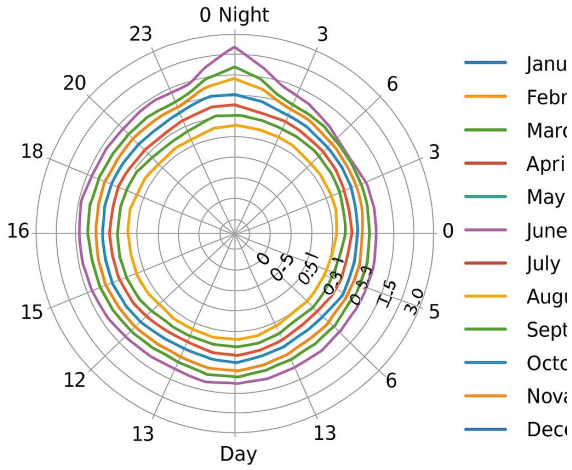

Figure 2. Hourly and monthly variation of wind speed at Sinjar region [36]

3. DESIGN OF WIND TURBINE BLADE

The findings of this research subject offer a comprehensive assessment of the design and assessment of a HAWT for a particular site in the Republic of Iraq. The concentration is on blade profiling and analysis through Computational Fluid Dynamics (CFD). Based on data analysis, the AMWS in Mosul, Iraq, is expected to be around 6 m/s per year. Therefore, the design wind speed is calculated with an empirical equation reaching the highest speed (1). Equation (2) is used to determine the square of the rotor diameter [6,7].

$$Ud = 1.4\,(AMWS) = 1.4(5) = 7\ m/s \quad (1)$$

$$D = 2\sqrt{P_d}/(0.5\,\rho\,\pi\,Cp\,U_d) \quad (2)$$

where D represents the rotor diameter. P_d is the power extracted by the turbine. ρ is the air density. C_p is the power coefficient. U_d is the wind speed.

The tip speed ratio is defined as the ratio of a wind turbine blade's tangential speed to the incident wind speed. For three-bladed horizontal-axis wind turbines (HAWT) commonly used in electricity generation, this ratio typically falls within the range of 4 to 10 [6, 37]. In this study, a design tip speed ratio of λ=7 has been selected. Table 1 summarizes the key design parameters for HAWT.

Table 1 Wind turbine design specifications

Design parameters	Symbol	Value	Unit
Rated power	P_d	100	W
Annual average wind speed	AMWS	5	m/s
Design wind speed	U_d	7	m/s
Rotor diameter	D	2	m
Power factor	Cpd	0.4	-
Number of blades	N_b	3	-
Number of elements	N_e	20	-

The data in Table 1 is based on assumptions tailored for a small-scale wind turbine, including a rated power of 100 W at a design wind speed of 7 m/s, reflecting typical conditions in moderate wind environments. The 2 m rotor diameter and three-blade configuration balance performance and structural considerations, while a power coefficient of 0.4 reflects expected aerodynamic efficiency. The number of elements (20) ensures accurate modeling of aerodynamic and structural properties.

In this study, the S809 airfoil was selected for the design and analysis of the wind turbine blade. The S809 airfoil was specifically designed for use in horizontal-axis wind turbines (HAWTs) as part of a collaborative research effort by the National Renewable Energy Laboratory (NREL). The selection of the S809 airfoil was based on several criteria, which were determined to optimize wind turbine performance, efficiency, and structural integrity. These criteria include high lift-to-drag ratio, stall delay characteristics, and structural integrity and thickness, and minimized noise.

The peak lift-to-drag ratio coefficient is 123.82 at a 7.5-degree angle of attack (α), with a lift coefficient of 1.276. Multiple theories are available for predicting aerodynamic performance and determining the ideal chord length and optimal twist angle distribution [23-26]. Among these, the simplest model, commonly attributed to Betz [27], is widely used in wind turbine blade design. This model disregards the impact of turbulence and rotational forces on the blade tip. The ideal rotor configuration

calculation, based on the Blade Element Momentum (BEM) method, involves dividing the blade into a specific number of sections. In this study, the blade is segmented into 20 equal parts, and equations (3-6) are applied to derive the ideal chord and twist distributions for each section [28]. For a three-bladed wind turbine designed for electrical applications, the tip speed ratio typically ranges between 4 and 10; therefore, a design tip speed ratio of 7 was chosen for this study.

$$\lambda r_{,i} = \lambda(r_i/R) \quad (3)$$

$$\emptyset i = (2/3)\ \tan^{-1}(1/\lambda r_i) \quad (4)$$

$$C_i = (8\pi r_i / N_b\ Cl_d)\ (1 - \cos \emptyset_i) \quad (5)$$

$$\theta_i = \emptyset_i - \alpha_d - \theta p{,}0 \quad (6)$$

$$C_p = P / 0.5\ \rho\ A\ V^3 \quad (7)$$

$$C_t = T / 0.5\ \rho\ A\ V^3 \quad (8)$$

where λ is the tip speed ratio. r_i is the radial position. R is the radius of the rotor. $\emptyset$ is the angle of attack. C_i is the aerodynamic force coefficient. N_b is the number of blades. Cl_d The lift coefficient at the radial position r_i. θ_i is the aerodynamic twist angle. αd is the design angle of attack. A is the sweep area. P is the pressure. T is the thrust. The twist angle (θi) denotes the variance between the flow angle and the design angle of attack at each blade element. Figs. 3 and 4 illustrate the optimal distribution of chords and twist angles at each blade element. Figure 5 shows the blade geometry.

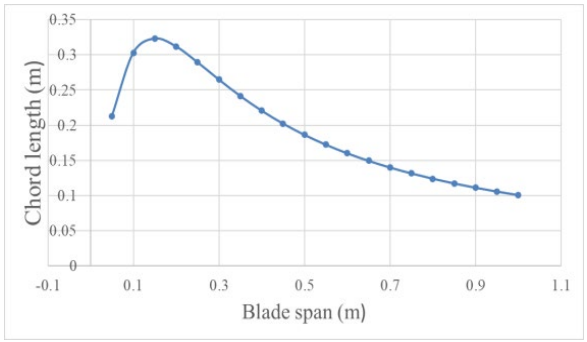

Figure 3. Distribution of the Chord length

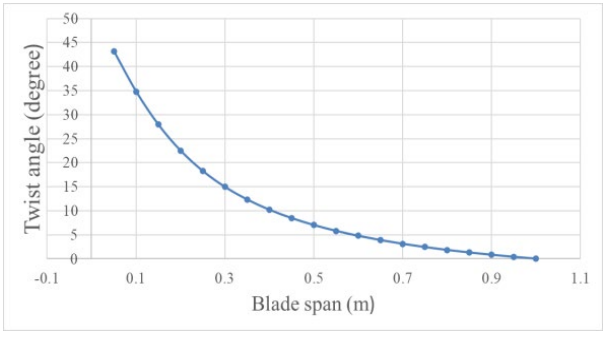

Figure 4. Distribution of the Twist angle

Figures 3 and 4 illustrate the blade profile distribution, specifically the chord length and twist angle along the blade span. The profiles were derived using Blade Element Momentum (BEM) theory, where the blade was segmented into twenty elements, with chord length and twist angle calculated for each segment.

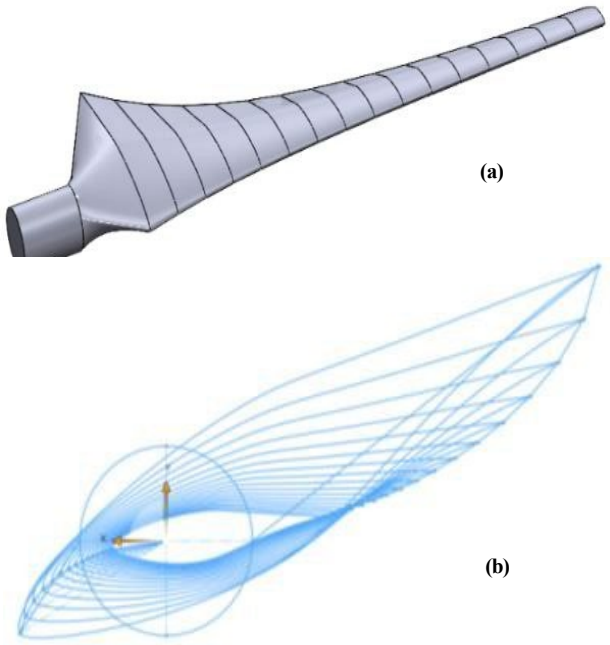

Figure 5. Blade geometry: (a) three-dimensional blade, (b) configurations of airfoils

4. NUMERICAL MODEL

This section presents the outcomes of the three-dimensional steady-state Computational Fluid Dynamics (CFD) simulations, including code validation, flow domain and boundary conditions, as well as the computational domain.

4.1. Code validation

The rotor blade from NREL Phase VI has been chosen for the validation test case for the CFD simulation in this study. The choice of the NREL Phase VI rotor blade model for CFD analysis of a wind turbine may be based on its extensive use as a benchmark in wind energy research due to the availability of high-quality experimental data. This model is well-documented, providing reliable validation data for computational studies, making it ideal for comparing numerical results with empirical measurements. Its comprehensive aerodynamic and structural characteristics offer a robust reference for evaluating turbine performance, making it a preferred option for accurate and validated CFD simulations. The NREL Phase VI unsteady aerodynamics experiments, referenced in studies [29, 30], were

extensively conducted at NASA Ames' wind tunnel facilities. This wind turbine is an upwind, two-bladed horizontal-axis wind turbine (HAWT) with tapered and twisted blades. The blades feature the S809 airfoil section from root to tip. Detailed specifications of the blade can be found in Table 2.

Table 2. NREL phase VI blade description

Description	Value	Unit
Number of blades	2	
Rotor diameter	10.06	m
Rotor speed	71.63	rpm
Rotor orientation	Upwind	
Blade tip pitch angle	3	degree
Blade profile	S809	
Blade chord length	0.358-0.728 (linearly tapered)	m
Blade twist angle	Non-linear twist along the span	

The aerodynamic rotor torque and thrust force were evaluated and compared with the experimental results reported by Hand et al. [31] and the CFD results presented by Li et al. [32] and Liu et al. [33].

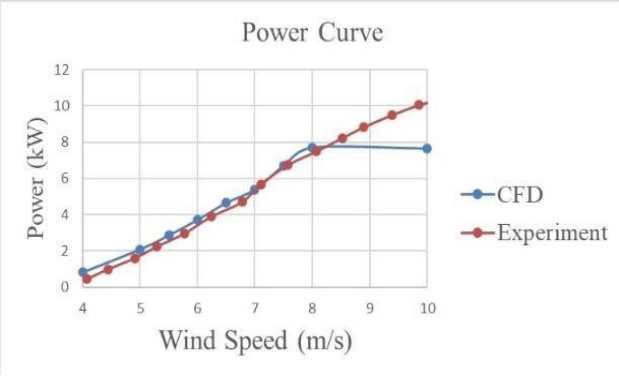

Figure 6. Comparison of power output between the present CFD and NREL-Experimental data

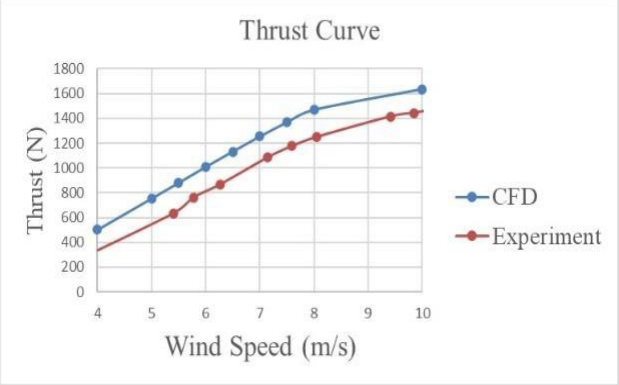

Figure 7. Comparison of thrust force between present CFD and NREL-Experimental data

The predicted outcomes in terms of aerodynamic power and thrust force align well with those from previous studies for wide range of wind speeds, as illustrated in Figs. 6 and 7. At a wind speed of 10 m/s, flow separation and stall conditions notably influenced the CFD predictions of aerodynamic thrust forces, leading to minor discrepancies between the CFD and experimental results at higher wind velocities.

4.2. Flow domain and boundary conditions

In this study, Ansys-CFX was utilized to analyze the wind turbine and the overall system design. The Moving Reference Frame (MRF) approach is used to simulate wind turbines because it allows for modeling the rotational motion of the turbine blades relative to a stationary frame of reference. This technique simplifies the simulation by treating the rotating region (e.g., rotor blades) as steady from its own perspective, while accounting for rotational effects when interacting with surrounding stationary air regions. The computational domain of the wind turbine is defined using the rotor radius (R) as the characteristic length, as shown in Figure 8. This domain consists of two subdomains: the rotating region, which includes the turbine blades, and the stationary region, encompassing the overall flow domain. Due to the significant impact of intense and helical vortices in the wake on the blade's aerodynamic characteristics [34], it is crucial to ensure the flow domain is sufficiently long to prevent aerodynamic interferences. Accordingly, the computational domain extends (5R) upstream of the turbine rotor, (10R) downstream, and (7R) in the cross-stream direction. Leveraging the 120-degree symmetry of the computational domain, only one of the three blades is explicitly simulated, with the others represented using periodic boundary conditions. This approach reduces computational complexity and cost while maintaining simulation accuracy [35, 36]. A constant wind velocity with a turbulent intensity of 5% is applied at the inlet boundary, and ambient pressure is set as the outlet condition downstream of the turbine rotor.

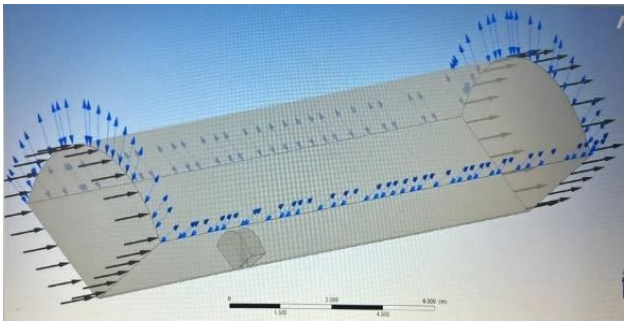

Figure 8. Flow domain and specified boundary conditions

All calculations were performed using the commercial software ANSYS (23R2) on a high-performance Lenovo gaming computer equipped with an Intel® Core™ i7-7700HQ processor (6M Cache, up to 3.80 GHz) and 16GB (2 x 8GB) DDR4 2400MHz SoDIMM memory.

4.3. Computational domain

Mesh generation is a fundamental step for numerically solving the governing equations of fluid mechanics within various physical domains. It involves discretizing the field into a collection of points (cells) that enable the approximation of partial differential equations by algebraic equations, which are then solved within the computational mesh domain. However, it is important to clarify that mesh generation itself is not a direct tool for solving these equations but rather a preparatory step essential for creating a structured computational space conducive to accurate numerical solutions.

The sensitivity test was performed to verify that the results from the CFD simulation are not dependent on the spatial mesh size [38, 39]. Figure 9 illustrates the relationship between torque and the number of mesh elements used in a mesh independence test. It shows that torque increases with the number of mesh elements up to a certain point, beyond which it begins to plateau. A mesh size of around 3,000,000 elements appears sufficient for accurate torque prediction, balancing accuracy with computational cost.

In this study, the mesh configuration depicted in Figure 10 incorporates a combination of structured and unstructured mesh elements to achieve local refinement where necessary. The mesh utilized trimmed cell hexahedrons in key regions, providing greater control over cell distribution and density. To enhance solution accuracy, fine mesh regions were employed around critical flow structures such as the blades and diffuser. This refinement aimed to capture unsteady flow behavior and improve the credibility of the analysis. In regions with high-gradient flow properties, particularly within boundary layers, prism layers were employed to achieve accurate wall treatment and flow resolution. Specifically, a total of 12 prism layers were generated near the blade and diffuser surfaces, with a cell growth ratio normal to the wall and first-layer thicknesses of 1.2 mm and 0.02 mm, respectively, to ensure proper boundary layer capture.

The computational mesh domain comprises two main finite volume regions: (1) the rotating domain, which includes the blades and hub, and (2) the stationary domain, which encompasses the diffuser structure, tower, and wind tunnel test section. These subdomains are connected through a sliding mesh interface, facilitating relative motion and accurate interaction between the rotating and stationary components.

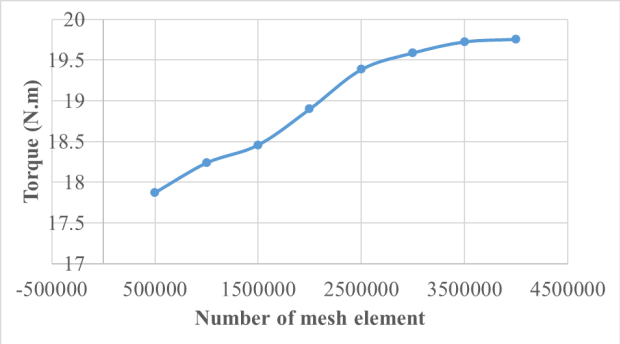

Figure 9. The relationship between torque and mesh size

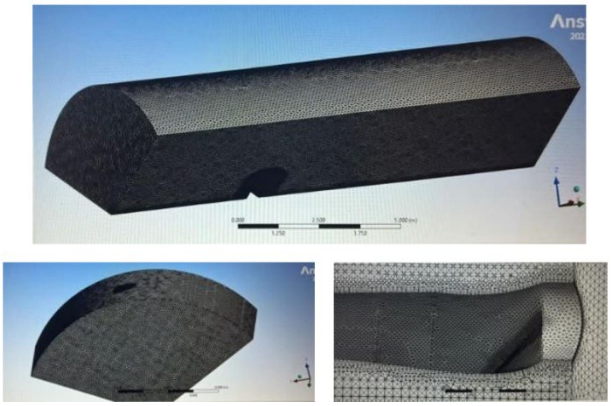

Figure 10. Tetrahedral computational domain

5. RESULTS AND DISCUSSION

Figure 11 illustrates the relationship between mechanical torque and incoming wind speed for a horizontal-axis wind turbine. The plot demonstrates a strong positive correlation, with torque increasing nearly linearly as wind speed rises, from approximately zero at 8 m/s to around 80 N·m at 20 m/s. This nearly linear trend is noteworthy, as it indicates that the turbine efficiently harnesses aerodynamic forces across the examined wind speed range without signs of saturation or aerodynamic inefficiency. This behavior underscores the effectiveness of the turbine's design in converting wind energy into mechanical energy, providing a foundation for optimizing turbine operation and control strategies.

Figure 12 depicts the fluctuation of power output with varying wind speeds. The power output increases significantly with wind speed, rising from negligible values at 8 m/s to approximately 4500 W at 20 m/s. This trend aligns with the theoretical power

relationship ($P \propto V^3$), demonstrating the expected cubic dependency of power on wind speed. However, the gradual rise in the power coefficient without evidence of saturation at higher speeds suggests that the turbine design minimizes aerodynamic loading and maintains efficiency across the tested range. This finding is critical, as it implies the turbine can sustain high energy conversion efficiency in areas with higher average wind speeds, maximizing energy generation.

The results from Figs. 11 and 12 collectively emphasize the importance of locating turbines in low-wind-speed regions to optimize energy output. Moreover, the absence of performance saturation at higher wind speeds suggests the potential for further operational optimization and scaling, enhancing the overall effectiveness of wind energy systems.

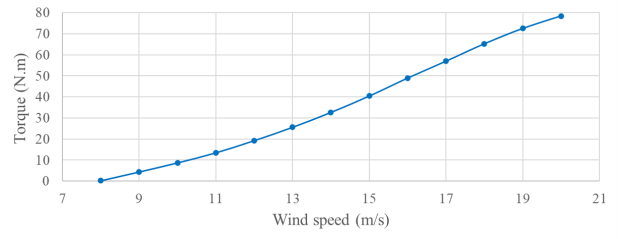

Figure 11. Variations of mechanical torque with incoming wind speed

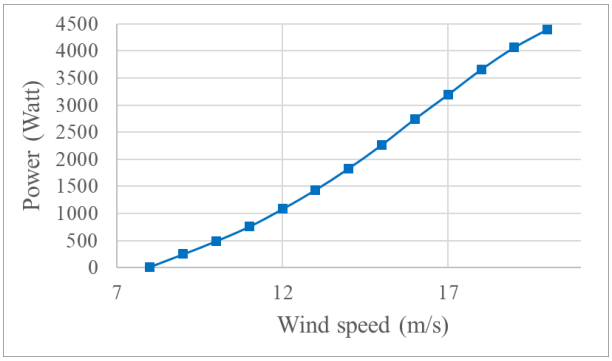

Figure 12. Variations of power with incoming wind speed

Figure 13 illustrates the relationship between the thrust force of a horizontal-axis wind turbine and the speed of the incoming wind. The thrust force shows a linear dependence on wind speed, starting from a small value at 8 m/s and reaching approximately 350 N at 20 m/s. This linear trend indicates that the aerodynamic forces acting on the turbine blades increase proportionally with wind speed, maintaining a consistent balance.

Thrust force serves as a primary load on the wind turbine structure, and its steady increase highlights the effective management of aerodynamic loads, particularly at higher gearing speeds. The monotonic trend and minimal oscillations observed in the data indicate that the tested wind turbine operates efficiently, without significant aerodynamic fluctuations, across the examined wind speed range [37]. These findings are valuable for engineers, as they provide insights into maintaining the structural integrity of wind turbines under varying wind conditions. The linear behavior of the thrust force also simplifies its estimation based on wind speed, aiding in the design and optimization of turbine components. This information is particularly useful for adapting wind turbine structures to dynamic wind environments and ensuring reliable performance.

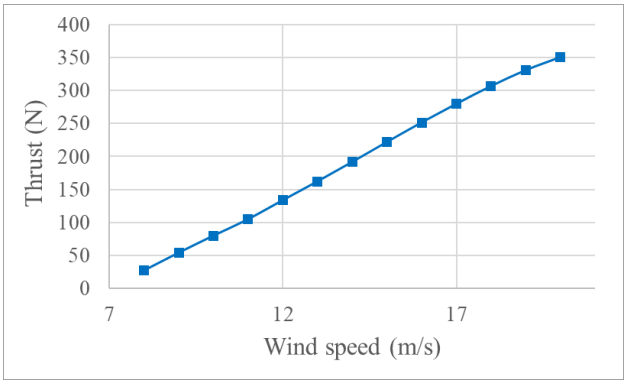

Figure 13. Variations of thrust force with incoming wind speed

Figures 14 and 15 illustrate the variations of the power coefficient (Cp) and thrust coefficient (Ct) as functions of the tip-speed ratio (TSR) for a horizontal-axis wind turbine. In Figure 13, the power coefficient (Cp) initially increases with TSR, peaking at around TSR=3.5TSR = 3.5TSR=3.5, where Cp reaches approximately 0.35. Beyond this point, Cp declines sharply, signifying that the turbine operates at its highest efficiency in converting wind energy into mechanical energy at this specific TSR. The sharp drop at higher TSR values reflects suboptimal blade performance, likely due to the imbalance between rotational speed and aerodynamic efficiency. Similarly, Figure 15 shows the thrust coefficient (Ct) peaking within the TSR range of approximately 4.0 to 4.5, with a maximum value of around 0.55. The decline in Ct beyond this range, though not shown here, is often linked to decreasing aerodynamic forces, potentially caused by blade stall or flow separation. The maximum Ct corresponds to the highest aerodynamic pressure exerted on the turbine blades, which is crucial for optimal energy harvesting. These results emphasize the importance of maintaining an appropriate TSR range (4.0–4.5) to achieve optimal turbine performance. The peaks observed in both Cp and Ct highlight the necessity of proper turbine regulation to maximize energy capture

while effectively managing thrust forces. Operating outside this range can lead to reduced efficiency and aerodynamic challenges, underscoring the critical role of maintaining the TSR at optimal levels for effective turbine operation.

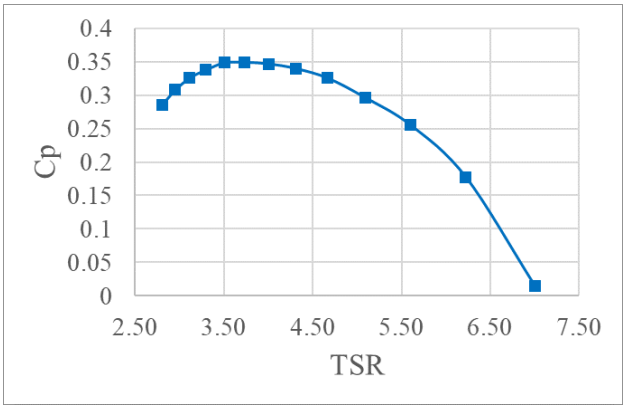

Figure 14. Power Coefficient as a Function of Tip-Speed Ratio (TSR)

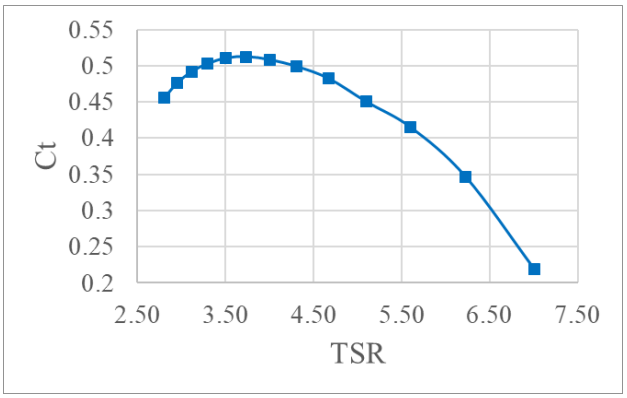

Figure 15. Thrust Coefficient as a Function of Tip-Speed Ratio (TSR)

Figure 16 illustrates the velocity field around a turbine blade, with wind speeds ranging from 8 to 20 m/s and span positions varying from 0.25 to 0.75. The contour plot shows the distribution of wind velocities, represented by a color gradient, with velocity vectors superimposed to indicate the flow direction and magnitude. The area immediately upstream of the blade exhibits a deceleration of the wind, as indicated by the transition from yellow to green hues. This deceleration is due to the aerodynamic drag and pressure buildup on the pressure side of the blade. In contrast, the downstream region shows a wake characterized by significantly lower wind speeds (depicted in blue and green), indicating energy extraction by the turbine. The flow acceleration around the blade's leading edge, visualized by the red and orange regions, signifies the high-speed flow resulting from the pressure difference created by the blade's shape and angle of attack (see Figure 16-a). The smooth flow lines around the blade depicted in Figure 16 indicate laminar flow conditions, which are essential for efficient aerodynamic performance. This figure underscores the significance of blade design in managing flow separation and wake effects, which are crucial for optimizing turbine performance and minimizing structural stresses.

The turbine blade velocity fields at a high wind speed of 20 m/s (span=25% and span=75%) are shown in Figure 15. As can be seen from the high wind speed, the wake region behind the blade's trailing edge is very severe, with a significant drop in flow velocity. The areas in blue and green show lower velocities as the blade extracts energy from this part of the flow, which is actually a good thing because turbine performance requires that, but more on it later. These wake effects are so pronounced that the design and layout of blades is crucial to controlling these wakes, as discussed in preceding posts on optimizing blade aeroelastic behavior for WFO systems (see More Eating Cake with Slim Sandwiches).

Examining the velocity contour plots, we can see that flow rates on the suction side of this blade exceed 40 m/s, and locations represented by red and orange regions are where the highest rate of acceleration takes place. Such acceleration represents the high-speed flow produced by the pressure differential that exists between two types of blade surfaces, which is essential in producing lift and therefore improving aerodynamic efficiency. Yet, poor flow separation can be noted on the aft section of the suction side at 50%, which presumably resulted from high turbulence intensity.

During the operation of a wind turbine, this separation can cause drag increases and lift losses that affect efficiency in general. Moreover, a splendid braking effect is observed on the pressure side close to the leading edge of the plate (the blue-green shades). This decrease in speed is indicative of the pressure rise that adds to lift generation, but stretches skin pressures and poses potential flow stability concerns. These flow phenomena are important to comprehend when designing blades, optimizing performance, and inherently ensuring that the turbine components remain in structural equilibrium during operation.

These velocity contours derive very important insights in terms of optimizing aerodynamic performance and structural durability for a horizontal-axis wind turbine. A study of the velocity distribution at different spans of a blade enables engineers to identify critical areas where flow separation is likely to happen and carry out a detailed analysis of how these separations would go on to impact efficiency and raise loads on structures. Such

variations identified permit blade geometry adjustments, viz., chord length and twist angle, to be made in blade design for optimized performance. Moreover, the data can aid in the development of blade designs of a turbine that would be more resistant to different aerodynamic forces it experiences at varying wind speeds and working conditions. An improved blade design is capable of enhancing capture efficiency, reducing mechanical fatigue, and increasing a turbine's lifespan. The developed velocity contours can be further used in developing advanced control strategies aimed at optimizing the operation of turbines, keeping them aligned with the wind direction and speed for maximum energy.

The contour plot of pressure around a turbine blade at a wind speed of 8 m/s, located radially at a span of 25%, is depicted in Figure 17-a. The contour plot shows distinct regions of upwind and downwind areas where there is a color gradient from yellow through green to blue, indicating a depression in pressure. This distribution of pressure aligns with the observed low power output at this wind speed, suggesting minimal aerodynamic lift generation. The relatively small pressure fall across the blade surfaces implies that the incoming wind energy is insufficient, creating a low-pressure difference between the blade faces. Consequently, the turbine operates inefficiently at this wind speed, converting wind energy to mechanical energy poorly. This confirms that the power output conditions at such low speeds are consistent with expectations, emphasizing the need for adequate wind speeds to optimize operation. The analysis of pressure contours at different spans and wind speeds is crucial in blade design and optimization, ensuring effective power recovery across a wide operational range.

As wind speed increases, a greater pressure gradient develops across the turbine blade, characterized by higher pressure on the windward side and a lower pressure on the leeward side. This variation significantly influences aerodynamic lift and improves power output. At a wind speed of 12 m/s, the pressure contours show a substantial pressure difference, reflecting an increase in aerodynamic forces acting on the blade. This rise in pressure directly correlates with increased power output, as depicted in Figure 17.

It underscores the potential of higher wind speeds to enhance energy conversion efficiency and optimize performance under strong wind conditions. Operating a wind turbine within its optimal wind speed range becomes paramount for maximizing energy capture and power generation. Engineers can leverage these findings to optimize blade design based on pressure contours at varying wind speeds, improving both performance and structural durability under diverse scenarios.

The maximum recorded pressure differential between the windward and leeward sides of the blade occurs at a wind speed of 20 m/s. However, this pressure difference decreases along the blade span, a critical factor for the structural integrity of the blade. Properly managing this pressure differential is essential to preventing structural failures and effectively handling torque, particularly at the blade tip. Careful consideration during the design phase is imperative to guarantee the structural integrity and operational reliability of the turbine under fluctuating wind conditions.

The contours of turbulent kinetic energy (TKE) at different wind speeds and blade spans are illustrated in Figure 18. At lower wind speeds (e.g., 8-10 m/s), TKE is predominantly generated behind the blade, on the windward and leeward sides, with increased turbulence behind the trailing edge, where wake forms. TKE increases linearly with blade span, reaching a maximum value of 20 m^2/s^2 at a wind speed of 8 m/s.

Although TKE rises with wind speed, a gradual increase on the leeward blade side indicates accelerated flow velocity and a larger velocity gradient across the blade surface. This significant velocity gradient is critical for converting kinetic energy into mechanical energy within the turbine. At higher wind speeds (e.g., 20 m/s), the behavior of TKE changes markedly.

Turbulent structures become more concentrated, contrasting sharply with lower wind speed scenarios. With increased stratification effects, maximum TKE regions form further away from the blade surface, particularly at a 50% span. This suggests a broader, more complex wake structure, with significant aerodynamic interactions. Enhanced TKE values in these areas can lead to higher energy distribution rates, impacting both efficiency and structural loading. This analysis further supports optimizing blade profiles to enhance energy capture. Improved blade design can ensure superior aerodynamic performance, enabling efficient turbine operation across a broader wind speed range.

Understanding TKE distribution is vital for designing robust turbine structures capable of handling dynamic turbulence-induced loads, maximizing energy capture, and maintaining structural integrity and longevity.

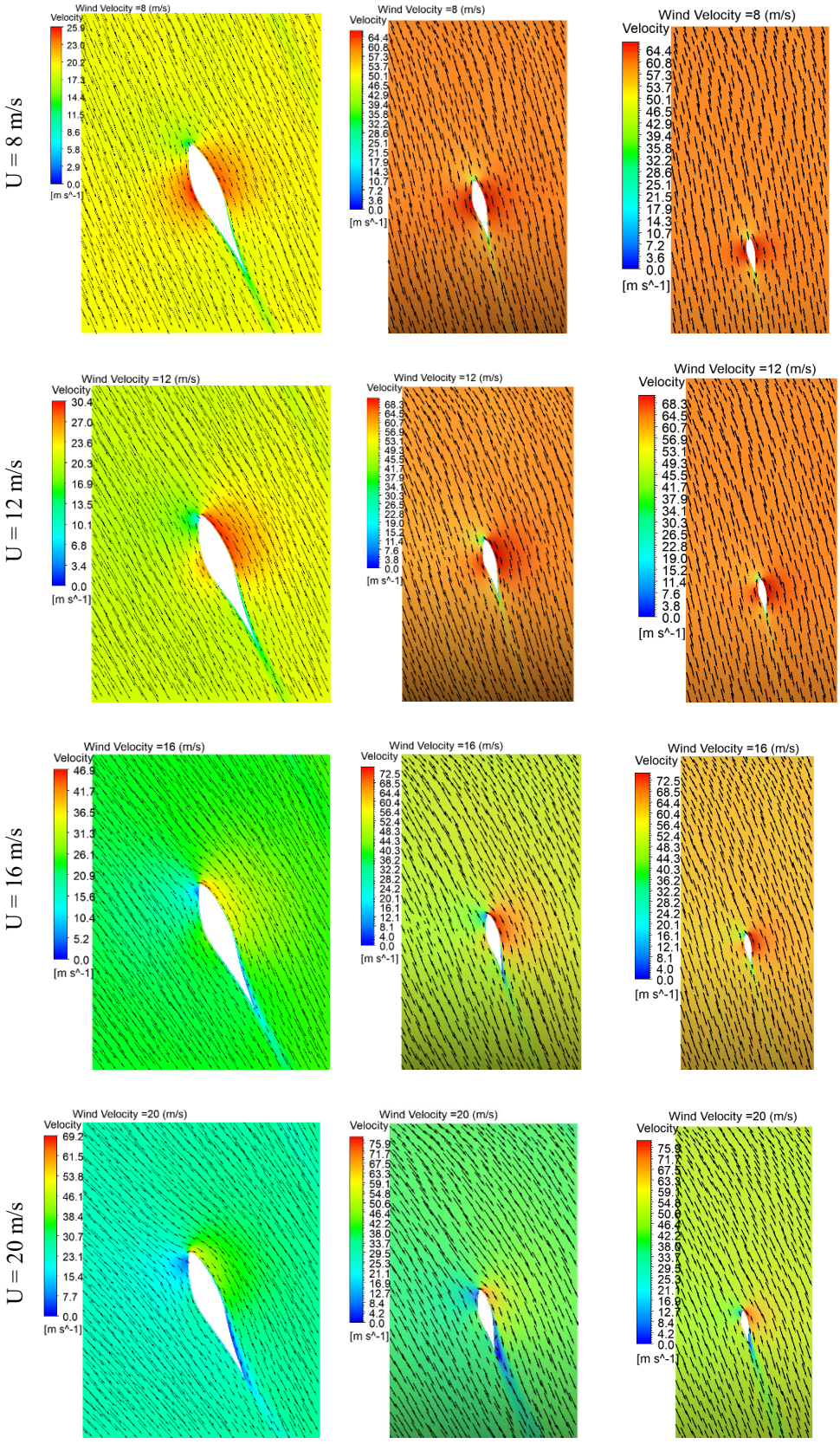

Figure 16. ISO-surface velocity contours at different blade span

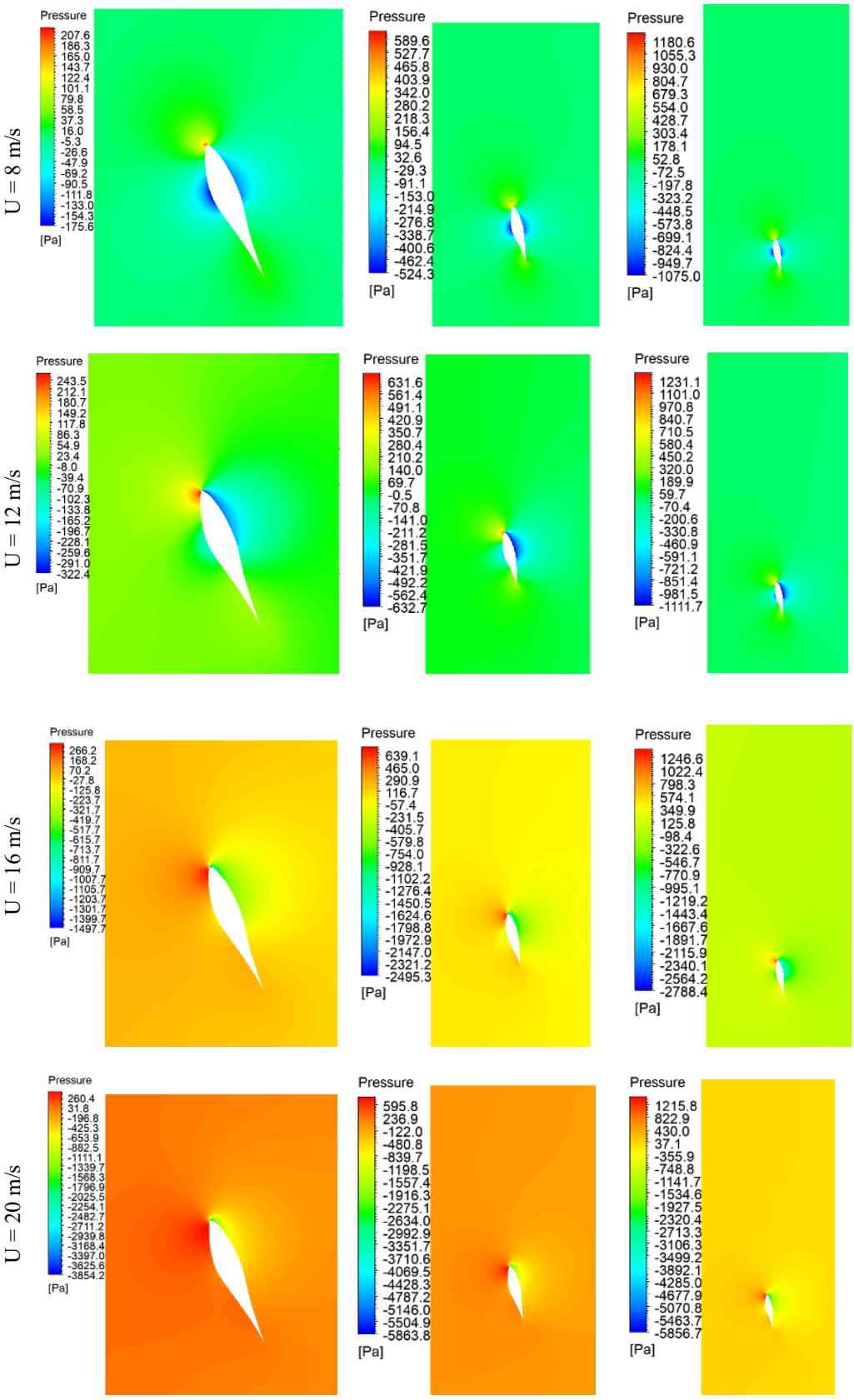

(a)Span = 0.25 (b)Span = 0.5 (c)Span = 0.75

Figure 17. ISO-surface pressure contours at different blade span

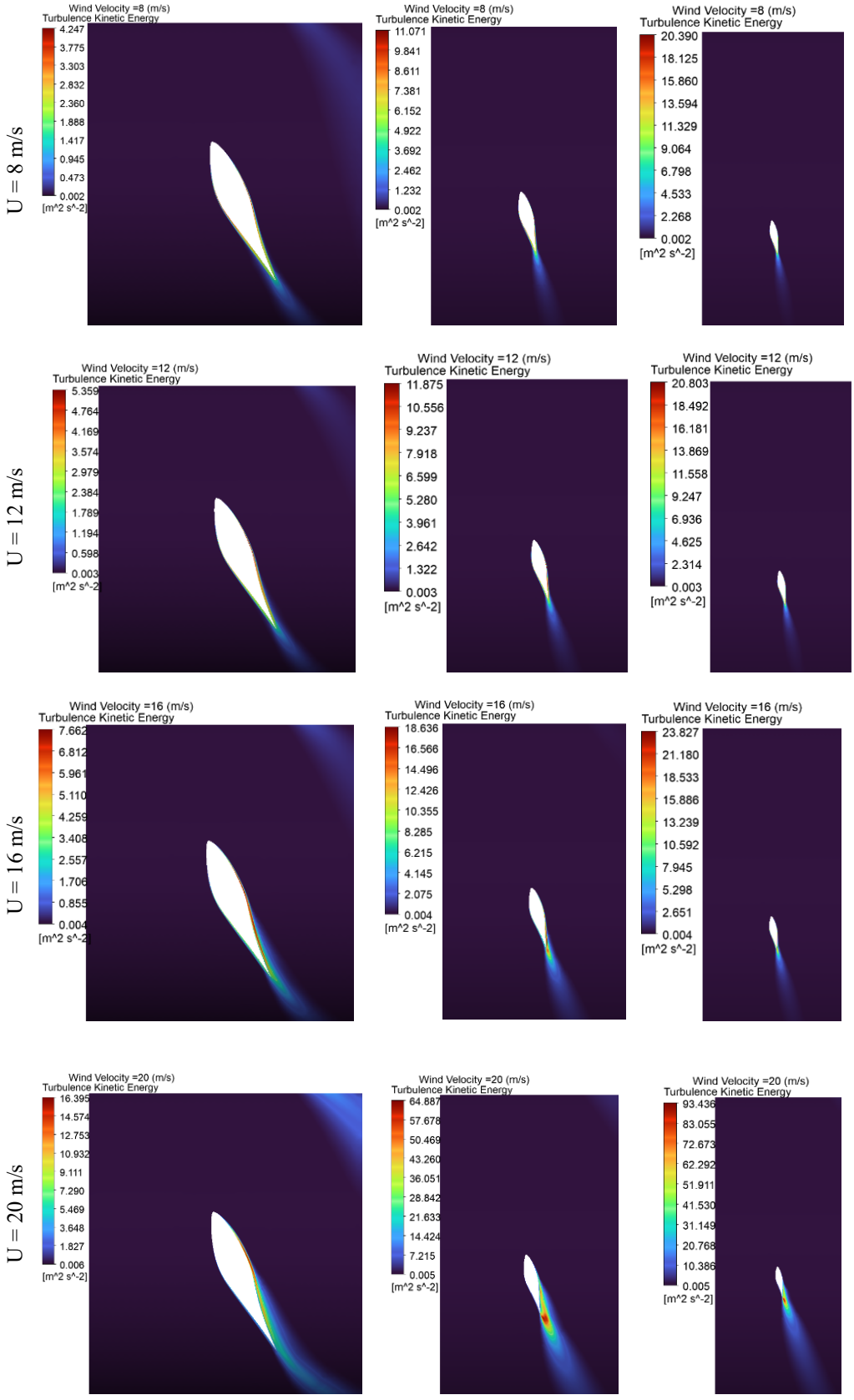

(a)Span = 0.25 (b)Span = 0.5 (c)Span = 0.75

Figure 18. ISO-surface turbulent kinetic energy contours at different blade span

6. CONCLUSION

This study presented a comprehensive Computational Fluid Dynamics (CFD) analysis and aerodynamic evaluation of a small-scale Horizontal Axis Wind Turbine (HAWT) specifically tailored to the meteorological conditions of Mosul City. By employing Blade Element Momentum (BEM) theory, the blade design was optimized through subdivision into twenty discrete elements, enabling precise determination of chord length and twist angle distribution along the span. The simulation results affirm the viability of the proposed blade design in enhancing energy capture and operational stability in low-wind-speed environments. The analysis revealed a strong correlation between power coefficient and tip speed ratio, with the coefficient reaching its maximum value of 0.35 at a tip speed ratio of 3.5. Beyond this point, a decline in performance was observed, indicating the importance of operating within optimal aerodynamic parameters.

The outcomes of this research underscore the potential for locally optimized small-scale wind turbines to contribute meaningfully to renewable energy solutions in urban settings with limited wind resources. The current HAWT design demonstrates promising performance in low-speed wind conditions, thereby offering a practical and efficient solution for decentralized clean energy generation in Mosul and similar regions.

While the present study successfully demonstrates the potential of using CFD and BEM theory for the aerodynamic optimization of a small-scale HAWT in low-wind-speed environments, certain limitations should be acknowledged.

Firstly, the simulations were based on idealized boundary conditions and steady-state assumptions, which may not fully capture the complexities of real-world wind behavior such as turbulence, gusts, or seasonal variability. Although the study utilized localized meteorological data, the dynamic fluctuations in wind patterns over time were not incorporated into the CFD model.

Secondly, the blade design was evaluated under a constant rotor speed, which does not account for variable-speed operations commonly found in practical wind turbine systems. This simplification may limit the generalizability of the results to real-world turbine performance under fluctuating operational conditions.

Lastly, experimental validation through wind tunnel testing or on-site deployment was not conducted. Although CFD provides valuable insight, empirical testing would enhance the credibility and applicability of the design for real-world implementation.

REFERENCES

[1] Edirisinghe DS, Yang H-S, Gunawardane SDGSP, Alkhabbaz A, Tongphong W, Yoon M, et al. Numerical and experimental investigation on water vortex power plant to recover the energy from industrial wastewater. Renew Energy 2023; 204:617–34. https://doi.org/10.1016/j.renene.2023.01.007.

[2] Yang H-S, Tongphong W, Ali A, Lee Y-H. Comparison of different fidelity hydrodynamic-aerodynamic coupled simulation code on the 10 MW semi-submersible type floating offshore wind turbine. Ocean Engineering 2023;281:114736. https://doi.org/10.1016/j.oceaneng.2023.114736.

[3] Yang H-S, Tongphong W, Ali A, Lee Y-H. Cross-comparison analysis of environmental load components in extreme conditions for pontoon-connected semi-submersible FOWT using CFD and potential-based tools. Ocean Engineering 2024;304:117248. https://doi.org/10.1016/j.oceaneng.2024.117248

[4] Yang H-S, Alkhabbaz A, Edirisinghe DS, Tongphong W, Lee Y-H. FOWT Stability Study According to Number of Columns Considering Amount of Materials Used. Energies (Basel) 2022; 15:1653. https://doi.org/10.3390/en15051653.

[5] Alkhabbaz A, Hamza H, Daabo AM, Yang H-S, Yoon M, Koprulu A, et al. The aero-hydrodynamic interference impact on the NREL 5-MW floating wind turbine experiencing surge motion. Ocean Engineering 2024;295:116970. https://doi.org/10.1016/j.oceaneng.2024.116970.

[6] Alkhabbaz A, Yang H-S, Weerakoon AHS, Lee Y-H. A novel linearization approach of chord and twist angle distribution for 10 kW horizontal axis wind turbine. Renew Energy 2021;178:1398–420. https://doi.org/10.1016/j.renene.2021.06.077.

[7] Alkhabbaz A, Yang H-S, Tongphong W, Lee Y-H. Impact of compact diffuser shroud on wind turbine aerodynamic performance: CFD and experimental investigations. Int J Mech Sci 2022;216:106978. https://doi.org/10.1016/j.ijmecsci.2021.106978.

[8] Edirisinghe DS, Yang H-S, Gunawardane SDGSP, Alkhabbaz A, Tongphong W, Yoon M, et al. Numerical and experimental investigation on water vortex power plant to recover the energy from industrial wastewater. Renew Energy 204:617–34 (2023).

[9] Kim IC, Alkhabbaz A, Jeong H, Lee YH. Optimization Methodology of Small Scale Horizontal Axis Shrouded Tidal Current Turbine. 2019 IEEE Asia-Pacific Conference on Computer Science and Data Engineering (CSDE), IEEE; 2019, p. 1–3.

[10] Ghalandari M, Mukhtar A, Yasir ASHM, Alkhabbaz A, Alviz-Meza A, Cárdenas-Escrocia Y, et al. Thermal conductivity improvement in a green building with Nano insulations using machine learning methods. Energy Reports 9:4781–8 (2023).

[11] R. V. Rodrigues and L. A. Rossi, "Performance of small wind turbines: simulation of electricity supply to loads connected to the public or isolated grid," *Eng. Agríc.*, vol. 36, pp. 281–290, Apr. 2016, doi: 10.1590/1809-4430-Eng.Agric.v36n2p281-290/2016.

[12] I. K. Wiratama, I. M. Mara, and I. Nuarsa, "Investigation of factors affecting power curve wind turbine blade," *J. Eng. Appl. Sci.*, vol. 11, pp. 2759–2762, Jan. 2016.

[13] S. Samah, S. Oudah, M. Salah, C. Author, Samah, and S. Oudah, "Preliminary investigation study of wind energy at Tuz-Khormatu in Iraq. *Private researcher in wind energy projects. **Ministry of Electricity/Iraq," Jun. 2016.
[14] R. Tariq Ahmed Hamdi and M. Abdul Hussein, "Modeling and Simulation of Wind Turbine Generator Using Matlab-Simulink," *J. Al-Rafidain Univ. Coll.*, vol. 40, pp. 282–300, Jan. 2017.
[15] Zhang, Z., Verma, A., & Kusiak, A. (2012). Fault analysis and condition monitoring of the wind turbine gearbox. IEEE Transactions on Energy Conversion, 27(2), 526–535. https://doi.org/10.1109/tec.2012.2189887
[16] M. Ibrahim, S. Fawaz, Abdullah, and B. Salih, "Modeling and Simulation of 1.5MW Wind Turbine," Jan. 2018.
[17] T. Burton, D. Sharpe, N. Jenkins, and E. Bossanyi, "Wind Energy Handbook," 2002.
[18] MR .Sitthichok Sitthiracha " An Analytical Model of Spark Ignition engine for performance prediction . king . Mongkut's Institute of technology North Bangkok .2006
[19] Danook, S., Tawfeeq, K., & Mansoor, E. (2018). Effect of moisture percentage on the wind turbine performance. Al-Kitab Journal for Pure Sciences, 2(1). https://doi.org/10.32441/kjps.v2i1.145
[20] Mammadov, E., Farrokhabadi, M., & Canizares, C. A. (2021). Ai-enabled predictive maintenance of wind generators. 2021 IEEE PES Innovative Smart Grid Technologies Europe (ISGT Europe), 1–5. https://doi.org/10.1109/isgteurope52324.2021.9640162
[21] Song, D., Zheng, S., Yang, S., Yang, J., Dong, M., Su, M., & Hoon Joo, Y. (2021). Annual energy production estimation for variable-speed wind turbine at high-altitude site. Journal of Modern Power Systems and Clean Energy, 9(3), 684–687. https://doi.org/10.35833/mpce.2019.000240
[22] Gharaibeh, A. A., Al-Shboul, D. A., Al-Rawabdeh, A. M., & Jaradat, R. A. (2021). Establishing regional power sustainability and feasibility using wind farm land-use optimization. Land, 10(5), 442. https://doi.org/10.3390/land10050442
[23] R. Gasch, J. Twele, Wind Power Plants:Fundamentals, Design, Construction and operation.2nd English Edition of the Standard German Textbook in its, fifth ed., 2012.
[24] M. Duquette, K. Visser, Numerical implications of solidity and blade number on rotor performance of horizontal-axis wind turbines, J. Sol. Energy Eng. 125 (2003) 425e432, https://doi.org/10.1115/1.1629751.
[25] J. Chattot, Optimization of wind turbines using helicoidal vortex model, J. Sol. Energy Eng. 125 (2003) 418e424, https://doi.org/10.1115/1.1621675.
[26] Prandtl L, Betz A, Vier Abhandlungen zur Hydromechanik und Aerodynamik. G€ottinger Klassiker Der Str€omungsmechanik Bd. 3, 1919 (in German).
[27] Manwell, J. F., McGowan, J. G., & Rogers, A. L. (2009). Wind Energy Explained: Theory, Design, and Application (2nd ed.). Wiley
[28] Hamzah H, Jasim L, Alkhabbaz A, Sahin B. Role of honeycomb in improving subsonic wind tunnel flow quality: numerical study based on orthogonal grid. J. mechanical Engineering Research and Developments 2021; 44:352 – 69.
[29] Liu Y, Xiao Q, Incecik A, Peyrard C, Wan D. Establishing a fully coupled CFD analysis tool for floating offshore wind turbines. Renewable Energy 2017;112: 280 – 301.
[30] Hand M. M., Simms D. A., Fingersh L. J., Jager D. W., Cotrell J. R., Schreck S., Larwood S. M., Unsteady Aerodynamics Experiment Phase VI: Wind Tunnel Test Configurations and Available Data Comparisons. NREL/TP-500-29955, 2001.
[31] Li Y, Paik K, Xing T, Carrica PM. Dynamic overset CFD simulations of wind turbine aerodynamics. Renewable Energy 2012;37:285 – 98.
[32] Liu Y, Xiao Q, Incecik A, Peyrard C, Wan D. Establishing a fully coupled CFD analysis tool for floating offshore wind turbines. Renewable Energy 2017;112: 280 – 301.
[33] J. Mo, A. Choudhry, M. Arjomandi, Y. Lee, Large eddy simulation of the wind turbine wake characteristics in the numerical wind tunnel model, J. Wind Eng. Ind. Aerod. 112 (2013) 11e24, https://doi.org/10.1016/j.jweia.2012.09.002.
[34] J. Mo, Y. Lee, CFD investigation on the aerodynamic characteristics of a small-sized wind turbine of NREL Phase VI operating with a stall-regulated method,J. Mech. Sci. Technol. 26 (2012) 81e92, https://doi.org/10.1007/s12206-011-1014-7.
[35] Jonkman, J., and Buhl, M., "Loads analysis of a floating wind turbine using fully coupled simulation
[36] Hassoon, Ahmed F. Determination trends and abnormal seasonal wind speed in Iraq. Iraq: N. p., 2013. Web.
[37] Mahmood, Y., Haddar, M., Taktak, M. (2024). Three Dimensional CFD Analysis of Horizontal Wind Turbine Designed for Mosul City Weather Conditions. In: Chouchane, M., et al. Design and Modeling of Mechanical Systems - VI. CMSM 2023. Lecture Notes in Mechanical Engineering. Springer, Cham. https://doi.org/10.1007/978-3-031-67152-4_19
[38] Alkhabbaz, A., Hamzah, H., Hamdoon, O. M., Yang, H.-S., Easa, H., & Lee, Y.-H. (2025). A unique design of a hybrid wave energy converter. Renewable Energy, 245, 122814. https://doi.org/10.1016/j.renene.2025.122814
[39] Yang, H.-S., Alkhabbaz, A., & Lee, Y.-H. (2025). Integrated CFD and hydrodynamic correction approach for load response analysis of floating offshore wind turbine. Ocean Engineering, 328, 121007. https://doi.org/10.1016/j.oceaneng.2025.121007